

Diel Variability Affects the Inorganic Marine Carbon System in the Sea-Surface Microlayer of a Mediterranean coastal area (Šibenik, Croatia)

5 Ander López-Puertas^{1,2}, Oliver Wurl¹, Sanja Frka³, Mariana Ribas-Ribas¹

¹ Center for Marine Sensors (ZfMarS), Institute for Chemistry and Biology of the Marine Environment (ICBM), School of Mathematics and Science, Carl von Ossietzky Universität Oldenburg, Ammerländer Heerstraße 114-118, 26129 Oldenburg, Germany

10 ² Instituto Universitario de Investigación Marina (INMAR), Universidad de Cádiz, 11510, Puerto Real, Cádiz, Spain

³ Laboratory for Marine and Atmospheric Biogeochemistry, Division for Marine and Environmental Research, Ruđer Bošković Institute, Bijenicka c. 54, 10000 Zagreb, Croatia

Correspondence to: Ander López-Puertas (ander.lopezpuertas@uca.es)

15 Abstract

The ocean plays a crucial role in the global carbon cycle by absorbing and storing about one-third of anthropogenic carbon dioxide (CO₂). It is estimated that the ocean has sequestered approximately 26% of CO₂ emissions over the last decade, resulting in significant changes in the marine carbon system and impacting the marine environment. The sea-surface microlayer (SML) plays a crucial role in these processes, facilitating the transfer of matter and energy between the ocean and the atmosphere. However, most studies on the carbon cycle in the SML have primarily addressed daily variability and overlooked nocturnal processes, which may lead to inaccurate global carbon estimates. We analysed temperature, salinity, pH_{T25}, and pCO₂ using data collected over three complete diel cycles during an oceanographic campaign along the Croatian coast near Šibenik in the Middle Adriatic. Our analysis revealed statistically significant differences ($p < 0.05$) between daytime and nighttime measurements of temperature, salinity, and pH_{T25}. These differences may be related to the occurrence of buoyancy fluxes, which are typically more pronounced during the day and could enhance CO₂ fluxes, as observed with values of $1.98 \pm 2.52 \text{ mmol cm}^{-2} \text{ h}^{-1}$ during the day, while at night, they dropped to $0.01 \pm 0.02 \text{ mmol cm}^{-2} \text{ h}^{-1}$. These findings emphasise the importance of considering complete diurnal cycles to accurately capture the variability in thermohaline features and carbon exchange processes, thereby improving our understanding of the ocean's role in climate change.

1. Introduction

The ocean is a crucial climate regulator that mitigates the effects of anthropogenic emissions (Gattuso *et al.*, 2015). It absorbs more than 90% of the Earth's excess heat (Hoegh-Guldberg *et al.*, 2014; Pörtner *et al.*, 2019) and captures approximately one-third of anthropogenic carbon dioxide (CO₂) emissions (Pörtner *et al.*, 2019;

35 Wong *et al.*, 2014). It is well known that CO₂ has a significant impact on seawater chemistry (Doney *et al.*,
2009; Gattuso *et al.*, 2015). It is estimated that the ocean has sequestered approximately 26% of global CO₂
emissions over the last decade (Friedlingstein *et al.*, 2024). Consequently, changes in the ocean environment
have exceeded the magnitude and rate of natural variation due to anthropogenic carbon perturbation over the last
millennia (Gattuso *et al.*, 2015). In this context, the marine carbon system undergoes substantial modifications,
40 resulting in various effects on the marine environment, including a decrease in pH levels (Doney *et al.*, 2009;
IPCC, 2023; Orr *et al.*, 2005). Therefore, understanding the evolving state of marine biogeochemistry in the
context of climate change is crucial, with a primary focus on the upper layers of the water column, which are
closely linked to ocean-atmosphere interactions.

In the ocean-atmosphere system, the sea-surface microlayer (SML) plays a vital role in transferring materials and
energy, such as heat, gases, and particles (Wurl *et al.*, 2019), which must pass through it (Frka *et al.*, 2009; Stolle
45 *et al.*, 2020). The SML is a distinctive and complex marine environment that represents the interfacial boundary
layer between the ocean and the atmosphere (Cunliffe *et al.*, 2013; Frka *et al.*, 2009; Wurl *et al.*, 2011). Its
thickness typically does not exceed 1000 µm, and it exhibits distinct biological and physicochemical properties
compared with the underlying water masses (Cunliffe *et al.*, 2013; Stolle *et al.*, 2020; Wurl *et al.*, 2011). Thus,
50 the SML experiences instantaneous meteorological forcing, such as solar radiation, wind, and atmospheric inputs
(Wurl *et al.*, 2019; Gassen *et al.*, 2023), which impacts the development of physical and biogeochemical
processes occurring in the underlying water (Engel *et al.*, 2017; Liss & Duce, 1997; Mustaffa *et al.*, 2018; Stolle
et al., 2020; Wurl *et al.*, 2017). These characteristics of the SML overlap with the growing interest in
oceanographic research to study the spatiotemporal variability of the marine carbon system (Cantoni *et al.*,
55 2016), as this layer is essential for understanding global marine biogeochemistry. However, to gain a
comprehensive spatiotemporal perspective on marine carbon chemistry processes, focusing on underexplored
fields, such as the role of nocturnal processes within the diel cycle, is crucial.

Daily variations force cyclic changes in chemistry (De Montety *et al.*, 2011), which are influenced by processes
such as photosynthesis, air-sea gas exchange, and various environmental conditions (e.g., light, temperature, and
60 nutrient availability) (Poulson & Sullivan, 2010). These processes directly affect the seawater pH by adding or
removing CO₂ from seawater (Poulson & Sullivan, 2010; Takahashi *et al.*, 2002). It is well known that
photosynthesis consumes CO₂ during the day, thereby reducing *p*CO₂ levels and consequently causing an
increase in pH (Cantoni *et al.*, 2012; Takahashi *et al.*, 2002). At night, the CO₂ produced by respiration tends to
be more constant and accumulates in the water column, leading to an increase in *p*CO₂ and a decrease in pH
65 (Cantoni *et al.*, 2012; Del Giorgio & Williams, 2005; Gattuso *et al.*, 1999; Shaw *et al.*, 2012). Although these
processes are significant for seawater chemistry, research has predominantly focused on diurnal processes. As a
result, the roles of respiration and other nocturnal processes in the SML remain largely unexplored (Yates *et al.*,
2007).

Within this framework, the Mediterranean Sea presents a unique research opportunity to investigate the
70 spatiotemporal variability of the marine carbon system. It is often referred to as a "laboratory basin"
(Bergamasco & Malanotte-Rizzoli, 2010; Robinson & Golnaraghi, 1994) because it enables us to approximate
processes occurring on a global scale within a shorter timeframe and smaller space (Álvarez *et al.*, 2014).
Despite representing 0.8% of the global ocean surface (Álvarez-Rodríguez, 2012), the Mediterranean Sea is

considered an important anthropogenic carbon storage (Álvarez *et al.*, 2014), as it absorbs a disproportionately larger amount of anthropogenic carbon compared to the global ocean (Hassoun *et al.*, 2015; Schneider *et al.*, 2010). Higher acidification ranges (-0.001 to -0.009 pH unit yr^{-1}) (Hassoun *et al.*, 2022) were measured and exceeded those measured in the Atlantic Ocean (-0.001 to -0.0026 pH unit yr^{-1}) (Takahashi *et al.*, 2014), in line with regional coastal studies showing strong acidification trends in the Mediterranean (Kapsenberg *et al.*, 2017). However, as explored in this study, the dynamics of biogeochemical processes in coastal regions are more complex than those in the open ocean (Borges, 2005). When examining oceanic regions, it is essential to recognise that daily variability has a profound impact on marine carbon chemistry.

This study emphasises the role of diel variability in thermohaline features and dynamics of the marine inorganic carbon cycle in the coastal region of the Mediterranean Sea (Šibenik, Croatia), thereby providing a comprehensive understanding of the processes that influence the complete diurnal cycle. Therefore, it is essential to incorporate nocturnal processes into global estimates of marine carbon cycle dynamics. We present high-resolution data to understand biogeochemical processes and their variability in the water column, which complicates predictions of variations in the coastal marine carbon system (Cantoni *et al.*, 2012). We have focused on understanding the nocturnal processes that affect the inorganic carbon system, thereby helping to clarify the uncertainties associated with this system. This study contributes to the identification of anthropogenic influences on the marine environment in the context of climate change.

2. Materials and Methods

2.1. Sampling Strategy and Seawater Analyses

Sampling was conducted in the lower estuary of the Krka River (central-eastern Adriatic), offshore in the St. Anthony Channel, near Šibenik (Figure 1). The estuary is highly stratified and exhibits microtidality, extending approximately 23 km inland, with depths increasing from less than 2 m at the head to around 42 m at the mouth (Cukrov *et al.*, 2024a; Prohić & Juračić, 1989). Similar to other Mediterranean estuaries, tidal ranges are small (0.2–0.5 m), resulting in minimal currents and stable vertical stratification, with freshwater or brackish water flowing over a lower marine layer (Cukrov *et al.*, 2024a). Average annual river discharge is $\sim 50 \text{ m}^3 \text{ s}^{-1}$, varying seasonally from ~ 5 to $480 \text{ m}^3 \text{ s}^{-1}$ (Bužančić *et al.*, 2016; Cukrov *et al.*, 2024b; Marcinek *et al.*, 2020). Previous studies in the area have reported that water residence times range from a few days in winter to several weeks in summer, depending on the hydrodynamics of the freshwater or marine layers (Cetinić *et al.*, 2006; Zutić & Legović, 1987). During the sampling period (August 10–15, 2020), precipitation was very low, averaging 1.4 mm over the first half of August (Croatian Meteorological and Hydrological Service (2020), consistent with the dry summer conditions typical for the region. This environment provided ideal stable conditions for assessing the daily variability of SML and ULW parameters with minimal interference from tides or precipitation.

Temperature, conductivity, and pH data from the SML were collected using sensors integrated in a flow-through system on the “Sea Surface Scanner (S^3)” (Ribas-Ribas *et al.*, 2017). The S^3 is a 4.5 m long and 2.2 m wide uncrewed catamaran, remotely piloted by radio control from a small support vessel. As specified in Ribas-Ribas *et al.*, (2017), the system features rotating glass discs on which the SML water adheres via surface tension. A set of scraping mechanisms on the immersed side collects the adhering water and transfers it to a closed, continuous-flow system, minimising atmospheric contact. Underlying water (ULW) was continuously collected

at a depth of 1 m through a rigid inlet pipe. Both SML and ULW water were pumped directly to the onboard sensor and sampler system (Table 1). In addition, the S³ carried an automated water collector (Table 1) with twenty-four 1-L polypropylene bottles, which could be filled remotely with SML or ULW water, allowing discrete samples to be collected during transects. Discrete samples for inorganic carbon parameters (DIC and TA) were collected separately in bottles (250 mL) directly from the S³ outlets, approached by the catamaran with the support zodiac, and immediately sealed to prevent atmospheric contamination.

Field deployments of the S³ were conducted six times per diel cycle between 10 and 15 August 2020, with each deployment lasting 30–45 minutes. Although the catamaran moved along short transects within the sampling area, for analytical purposes, the sampling location was treated as a single point, since spatial variations within the region were minimal. Sensors recorded temperature, conductivity, and pH from both SML and ULW at 30-second intervals. Specifically, the pH was measured using the integrated sensor of the S³ flow-through system (Ribas-Ribas *et al.*, 2017) and is reported on the total scale. The uncertainties of the measured temperature, conductivity and pH were estimated based on sensor specifications (Table 1). Solar radiance and wind data were collected from a meteorological station (Davis Instruments, Vantage Pro2 Plus) located on Zlarin Island. For the analysis, a total of three diurnal cycles were sampled. In each cycle, four deployments were conducted during daytime conditions (diurnal data), and two deployments were performed at night (nocturnal data). Environmental conditions during the campaign were typical for the region, with no significant rainfall events. This deployment strategy enabled representative sampling of the study area while minimising the potential influence of microtidal variations on the SML and ULW measurements.

Subsamples from the SML and ULW were collected in high-density polyethylene (HDPE) bottles to determine the phosphate (PO₄³⁻) and silicate [Si(OH)₄] concentrations. To preserve the samples, mercury chloride (HgCl₂) was added. The preserved samples were stored at +4 °C until further analysis in the laboratory. Nutrient concentrations were measured using a sequential automatic analyser (SAA, SYSTEAM EASYCHEM) according to the standard protocols described by Laskov *et al.*, (2007) and Fanning & Pilson, (1973). These nutrient data were subsequently used as inputs for calculating partial pressure of CO₂ (pCO₂) with the CO₂Sys program (Version v3.2.0, MATLAB) (Sharp *et al.*, 2020; Van Heuven *et al.*, 2011).

Table 1. Manufacturers, models, and specifications of the sensors employed to measure pH, salinity, and temperature in the sea-surface microlayer (SML) and underlying water (ULW). Adapted from Ribas-Ribas *et al.*, (2017).

| Parameter | Manufacturer | Model | Range, unit, and resolution | Accuracy | Sample |
|-------------|--------------|-----------|-----------------------------|----------|-------------|
| pH | VWR | MU 6100 H | -2.000 to 19.999 | ± 0.005 | SML and ULW |
| Salinity | VWR | MU 6100 H | 0.0-70.0 | ±0.2% | SML and ULW |
| Temperature | VWR | MU 6100 H | -5.0° to 105.0°C | ±0.1°C | SML and ULW |

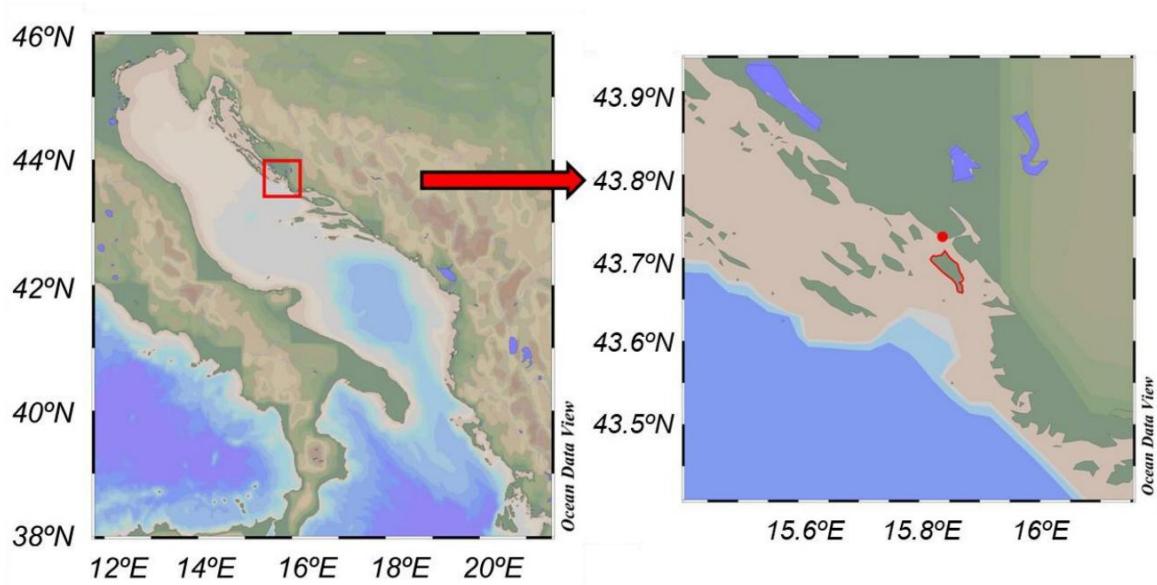


Figure 1. Map of the sampling area in the Middle Adriatic Sea, created using Ocean Data View (Schlitzer, 2022). The red dot indicates the sampling area, whereas Zlarin Island, where the meteorological station is situated, is outlined in red.

2.2. Marine Carbon System Determination

DIC samples (20 mL) were analysed by coulometric titration (CM 5014, UIC, USA) with an excess of 10% phosphoric acid. Total Alkalinity (TA) samples (100 mL) were measured via potentiometric titration (916 Ti-Touch, Metrohm, Switzerland) and calculated using a modified Gran plot approach implemented in Calculate (version 1.8.0) (Humphreys *et al.*, 2022). Calibration was performed with certified reference material (Batch 187) obtained from A. G. Dickson at the Scripps Institution of Oceanography. The 1σ measurement precision was $\pm 3 \mu\text{mol kg}^{-1}$ for DIC and $\pm 2 \mu\text{mol kg}^{-1}$ for TA.

To eliminate the effects of temperature variation on the results, the pH values measured in the seawater samples were adjusted to the average temperature value of 25.43 °C, hereafter referred to as pH_{T25} . The normalisation utilised an adjustment factor of 0.018 pH units per °C, which is widely accepted for the range of pH and TA conditions typical of seawater (Eq. 1) (Dickson *et al.*, 2007; Dickson & Millero, 1987; Zeebe & Wolf-Gladrow, 2001):

$$\text{pH}_{T25} = \text{pH} + (T - 25.43) \cdot 0.018 \quad (1)$$

To evaluate the marine carbon system, $p\text{CO}_2$ was calculated with the CO2SYS program (Version v3.2.0, MATLAB) (Sharp *et al.*, 2020; Van Heuven *et al.*, 2011) using as input parameters: DIC; TA, PO_4^{3-} , and Si(OH)_4 ; salinity (S); temperature (T), and pressure. The respective dissociation constants were used for carbon (Mehrbach *et al.*, 1973), sulfate (KSO_4) (Dickson & Millero, 1987), fluorine (KF) (Perez & Fraga, 1987), and the borate-salinity ratio (Lee *et al.*, 2010). Missing $p\text{CO}_2$ values were due to erroneous DIC and/or TA measurements. Consequently, standard deviations could not be calculated when the number of reliable data points was less than three. Once the $p\text{CO}_2$ values were calculated, the CO_2 flux through the ocean-atmosphere interface in the monitoring area was estimated using the following equation:

$$F = \Delta pCO_2 \cdot k \cdot \alpha \quad (2)$$

where F is the CO_2 flux ($mmol\ m^{-2}\ d^{-1}$), ΔpCO_2 is equal to the difference in the partial pressures of the gas between the surface water and the atmosphere, k is the gas transfer coefficient ($cm\ h^{-1}$) from Wanninkhof, (2014), and α is the solubility of CO_2 in seawater ($mol\ L^{-1}\ atm^{-1}$). To calculate the partial pressure gradient of CO_2 , atmospheric pCO_2 data were obtained as the monthly mean for August 2020 from the ICOS Lampedusa atmospheric station, which provides quality-controlled dry-air CO_2 measurements representative of the Mediterranean region (Pecci et al., 2023). To quantify the bias introduced when nocturnal fluxes were ignored, we compared daily means including all valid data from each cycle with means based only on daytime measurements. The percentage error was defined as $\left(\frac{F_{daytime} - F_{diel}}{F_{diel}}\right) \times 100$, with both means calculated as arithmetic averages of available fluxes. This approach explicitly evaluates the uncertainty in daily estimates when nocturnal processes are excluded (Garbe et al., 2014).

2.3. Salinity and density correction

To ensure high-quality data, a correction factor (CF) was applied to the continuous salinity and pH_{T25} data. Discrete salinity values obtained from laboratory analyses served as reference points and were compared to the average continuous values recorded by the S^3 (Ribas-Ribas et al., 2017). This process resulted in the derivation of distinct CFs, which were applied at each depth and during each time interval of the S^3 measurements (Ribas-Ribas et al., 2017). Once the salinity values were corrected, the pH was calculated using the CO2Sys program (Version v3.2.0, MATLAB) (Sharp et al., 2020; Van Heuven et al., 2011). These calculated pH_{T25} values were then utilised as reference points for comparison with the average continuous values obtained from the S^3 measurements (Ribas-Ribas et al., 2017). After correcting for salinity, the density (ρ) was calculated using the TEOS-10 (<https://www.teos-10.org/index.htm>) equation of state in RStudio (Team, 2023) based on the observed temperature and salinity values. From this calculation, sigma- t was defined as the density at a given temperature and salinity minus $1,000\ kg\ m^{-3}$. The propagated uncertainties for sigma- t and pCO_2 were estimated from the measurement precisions of temperature, salinity, pH, DIC, and TA. These estimates provide a quantitative basis for evaluating the reliability of calculated variables in subsequent analyses.

2.4. Evaporation rate calculation

The evaporation rate (E) was estimated using the following formula, which relates the latent heat flux (Q_E) (Brutsaert, 2013), the latent heat of vaporisation (L_v) (Kittel & Kroemer, 1980), and the calculated density of seawater (ρ):

$$E = \frac{Q_E}{L_v \cdot \rho} \quad (3)$$

2.5. Statistical Analysis

Since the assumptions of normality and homoscedasticity were not met for the collected data, the Kruskal-Wallis test was chosen as a nonparametric alternative to ANOVA. This test revealed significant differences between the data collected during the day and night, as well as between the SML and ULW, and among the medians of the cycles studied. A significance level (α) of 0.05 was established to determine whether the groups differed significantly. All statistical analyses were performed using RStudio (Team, 2023). In addition, to carry out a

complete analysis of the variability of the marine carbon system during the study period, anomalies in temperature, salinity, pH_{T25} , and pCO_2 data were calculated using the following expression: $\Delta(\text{SML} - \text{ULW})$. These differences were calculated for diurnal and nocturnal data for each cycle.

3. Results

The primary objective of this study was to understand the typical patterns of diurnal variability and depth-related differences in marine biogeochemistry during the observed cycles. Data on temperature, salinity, pH_{T25} , and pCO_2 were used to perform a statistical analysis of the similarity between the data collected during the diel cycle and to calculate the differences between the values measured in the SML and ULW. Additionally, we examined the temporal distribution using box-and-whisker plots and calculated the air-sea CO_2 exchange across the SML.

3.1. Meteorological conditions

To study the potential variance in the meteorological forcing observed during the observations, time-series graphs were plotted for solar radiation and wind speed (Figure 2). A consistent pattern of solar radiation was observed during all three cycles, with peaks of 525, 404, and 420 W m^{-2} observed at 14:00 UTC. Relatively low wind speeds were recorded during the day in all three cycles, averaging $1.26 \pm 1.46 \text{ m s}^{-1}$. Maximum wind speeds were observed at 14:00 and 18:00 UTC, higher for Cycles 1 and 2 (2.14 m s^{-1} and 5.22 m s^{-1}) than during Cycle 3 (0.95 m s^{-1}). Additionally, a decrease in wind speed was observed throughout the night, approaching near-zero values, except during Cycle 3, when the wind speed remained consistently close to zero.

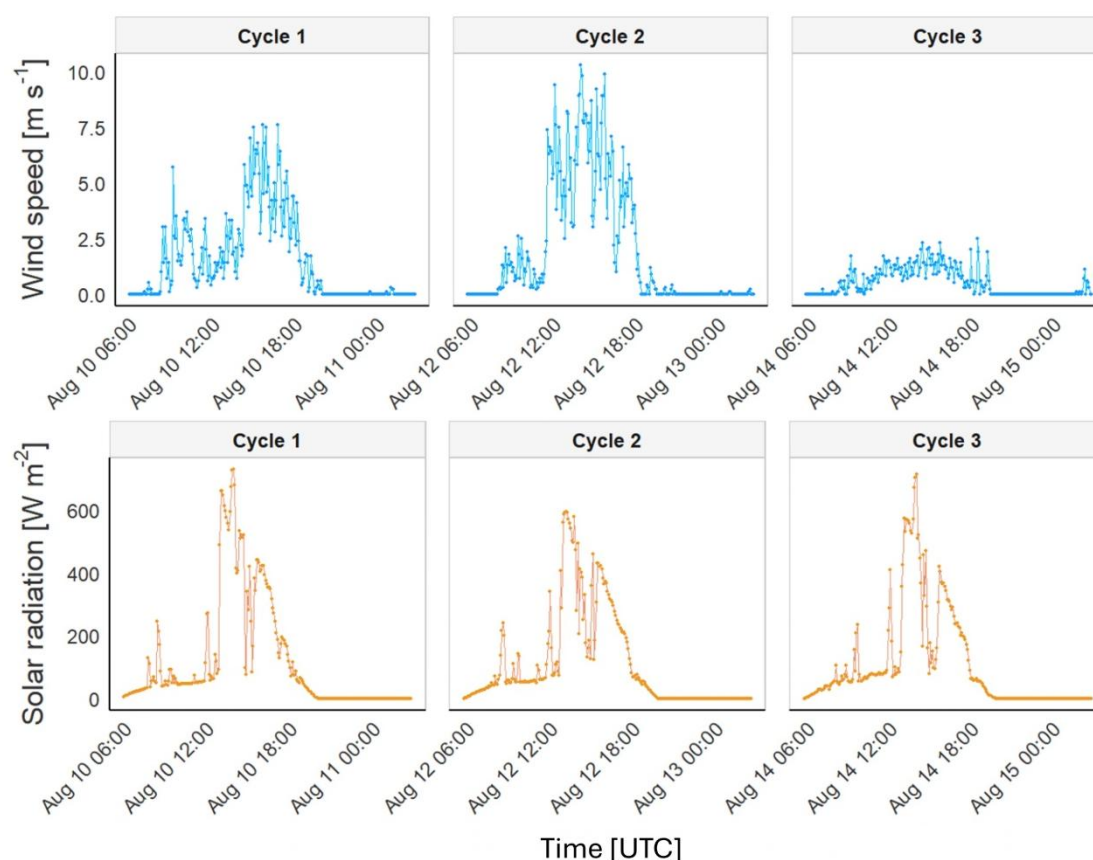


Figure 2. Time series showing wind speed and solar radiation on Zlarin Island (Figure 1) during the three studied cycles.

3.2. Daily trends

220 To investigate the overall distribution of physicochemical parameters throughout the daily sampling period at the SML and ULW, we show box-and-whisker plots for temperature, salinity, and pH_{T25} across different time intervals (Figure 3). We also performed the Kruskal-Wallis test to determine statistically significant differences (see section 2.5, Materials and Methods) between the SML and ULW (Table S1). The analysis revealed no significant temperature differences between the two depths during Cycle 1 (SML: 25.00 ± 0.85 °C; ULW: 225 24.90 ± 0.72 °C) and Cycle 2 (SML: 25.40 ± 0.62 °C; ULW: 25.40 ± 0.83 °C). However, in Cycle 3, ULW was slightly warmer, with a mean temperature of 26.60 ± 0.72 °C compared to 26.20 ± 1.20 °C in the SML. For salinity, significant differences were detected between SML and ULW during Cycles 1 and 2, with ULW exhibiting higher salinity levels in Cycle 1 (SML: 38.90 ± 0.32 g kg⁻¹; ULW: 39.10 ± 0.32 g kg⁻¹) and in Cycle 2 (SML: 39.2 ± 0.27 g kg⁻¹; ULW: 39.4 ± 0.29 g kg⁻¹). Notably, the salinity data showed greater variability, 230 especially in Cycle 2, in the SML, whereas the ULW remained relatively constant. The pH_{T25} data collected over the three cycles displayed considerable variability, with fluctuations observed throughout the day. The SML and ULW data showed significant differences during the first two cycles, with slightly higher values in the SML for Cycle 1 (SML: 8.030 ± 0.020 ; ULW: 8.020 ± 0.033) and for Cycle 2 (SML: 8.020 ± 0.020 ; ULW: 8.010 ± 0.024). No significant differences were observed in Cycle 3 (SML: 8.020 ± 0.032 ; ULW: 8.020 ± 0.032).

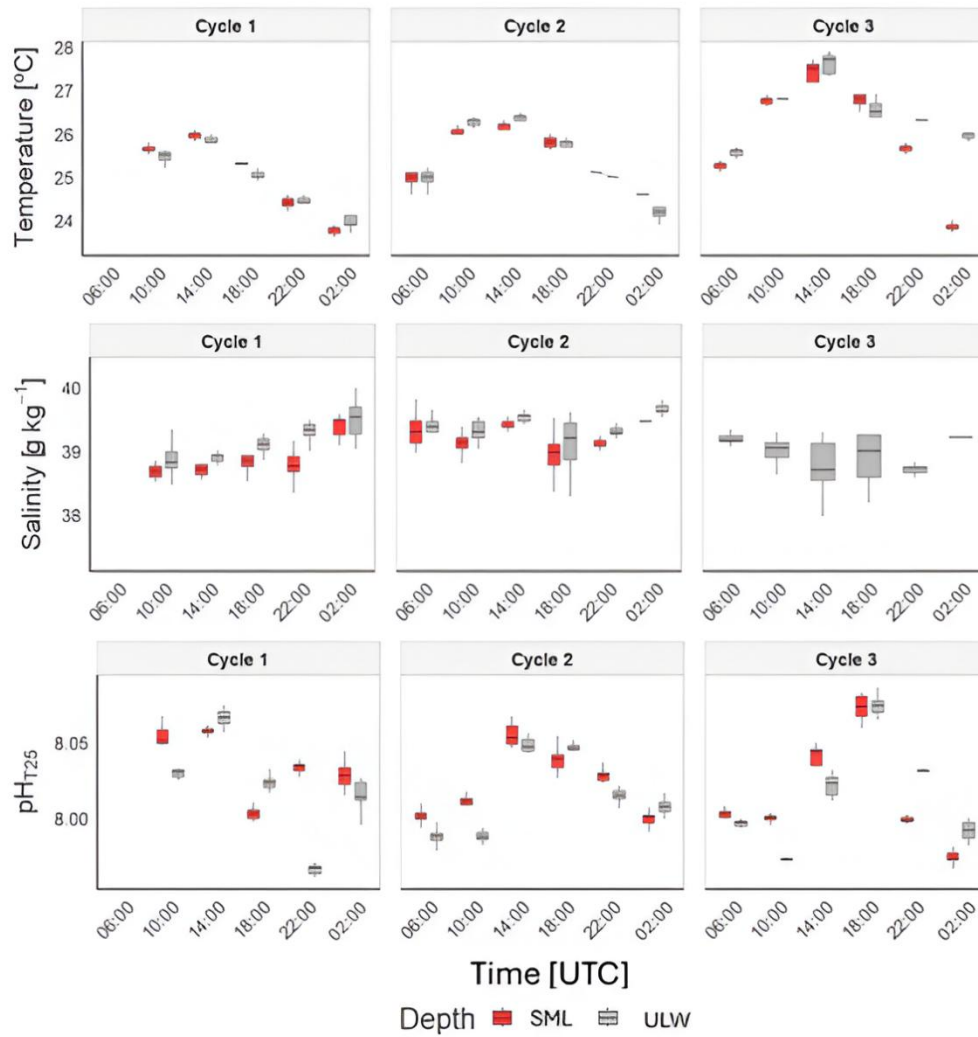


Figure 3. Box-and-whisker plots for the different time steps at which measurements were obtained at both the SML and ULW for temperature, salinity, and pH_{T25} . Each boxplot represents all measurements obtained during a single 30–45 minute deployment (data collected at 30-second intervals), with four daytime and two nighttime deployments per cycle. The horizontal line within each box denotes the mean of the data, whereas the vertical line associated with each box represents the 25th and 75th percentiles (Q1 and Q3) of the data.

3.3. Diel variability and depth-related anomalies

To assess diel variability in the marine carbon system, we statistically compared the thermohaline and key carbon cycle variables, pH_{T25} and pCO_2 , between day and night in the SML and ULW (Figure 4, Table 2). Additionally, we calculated $\Delta\text{SML-ULW}$ to evaluate the magnitude of vertical anomalies during diurnal and nocturnal conditions. The analysis of thermohaline variables indicated significant differences between diurnal and nocturnal data at the two depths across the three cycles (Table S2). However, the salinity data recorded from ULW during Cycle 3 did not exhibit significant differences. The observed anomalies between the SML and ULW varied across the three cycles for temperature. In Cycle 1, the SML experienced positive diurnal and negative nocturnal temperature anomalies on average (0.19 ± 0.14 ; -0.10 ± 0.14 °C). During Cycle 2, negative diurnal SML anomalies and positive nocturnal anomalies were observed (-0.13 ± 0.12 ; 0.28 ± 0.18 °C). In Cycle 3, diurnal and nocturnal SML negative anomalies were detected at -0.08 ± 0.24 and -1.34 ± 0.77 °C, respectively. Likewise, it was noted that salinity anomalies in SML were negative in Cycles 1 and 2, both for diurnal

(-0.23 ± 0.17 ; -0.14 ± 0.19 g kg⁻¹) and nocturnal data (-0.29 ± 0.30 ; -0.15 ± 0.29 g kg⁻¹). These results suggest that external factors may influence thermohaline variables, affecting the pronounced temporal distribution of the diel cycle.

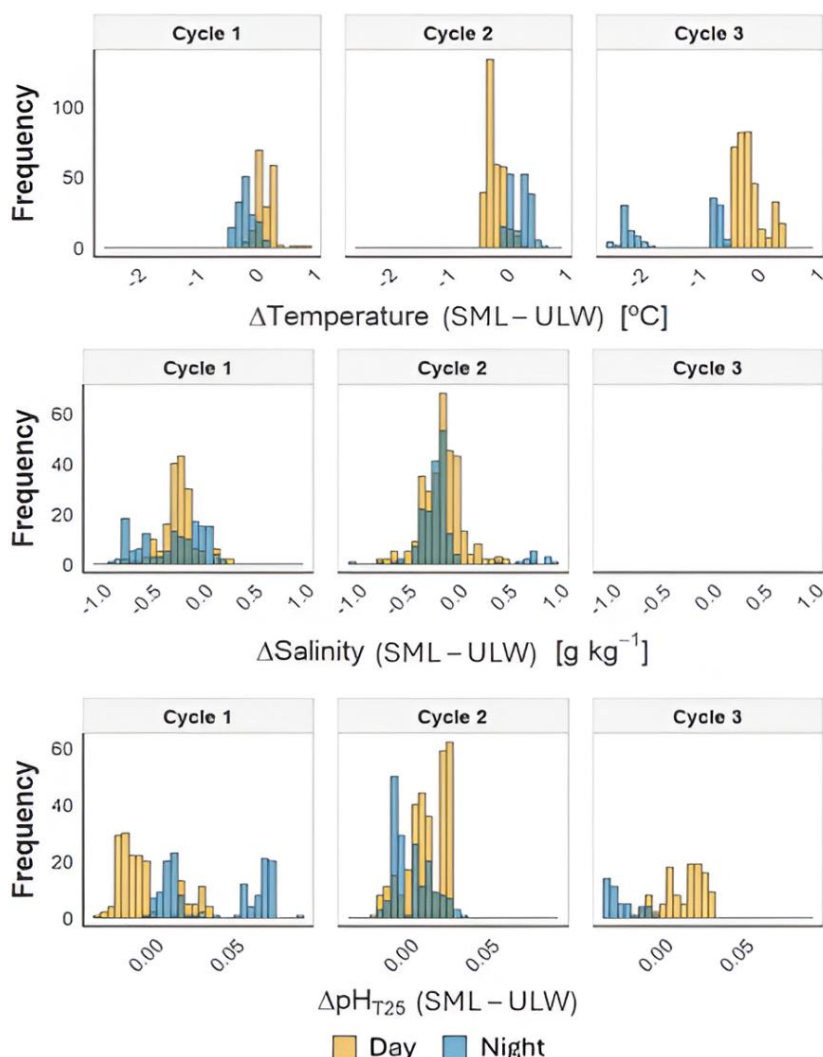


Figure 4. Frequency distribution of the anomaly of temperature, salinity, and pH_{T25} between SML and ULW observed during the day (orange) and at night (blue) across the three cycles studied.

When comparing the diurnal and nocturnal data for the variables associated with the marine carbon system at each depth (Table S2), we found significant differences in pH_{T25}, except for the ULW data during Cycle 3. However, no significant differences were observed in the *p*CO₂ data. The pH_{T25} deltas (Table 2) revealed that during Cycle 1, lower pH_{T25} values were recorded in the SML for diurnal data and higher for nocturnal data (-0.006 ± 0.018 ; 0.038 ± 0.029). During Cycle 2, the SML showed higher diurnal (0.011 ± 0.012) and lower nocturnal (-0.002 ± 0.012) pH_{T25} values. Meanwhile, for Cycle 3, the SML indicated higher pH_{T25} values for the diurnal data (0.013 ± 0.012) and lower values for the nocturnal data (0.026 ± 0.009) (Table 2). For the *p*CO₂ data during Cycles 1 and 3, lower *p*CO₂ values were recorded in the SML during both diurnal (-11 ± 56 μatm and -22 ± 22 μatm, respectively) and nocturnal periods (-4 and -8 μatm, respectively) (Table 2). In Cycle 2, lower diurnal and higher nocturnal values were observed in the SML, with values of -12 ± 19 μatm and 7 μatm, respectively. The large variability between the nighttime and daytime data distributions at the two depths can be

attributed to the complex interaction between biological processes and atmospheric and oceanic forcing, such as heat flux and mixing processes.

Table 2. Mean anomalies of temperature, salinity, pH_{T25}, and pCO₂ between the two depths studied (Δ (SML-ULW)).

| | | Temperature [°C] | | Salinity [g kg ⁻¹] | | pH _{T25} | | pCO ₂ [µatm] | |
|---------|-------|------------------|------------------|--------------------------------|------------------|-------------------|------------------|-------------------------|------------------|
| | | n | Δ SML-ULW | n | Δ SML-ULW | n | Δ SML-ULW | n | Δ SML-ULW |
| Cycle 1 | Day | 177 | 0.19 ± 0.14 | 606 | -0.23 ± 0.17 | 175 | -0.006 ± 0.018 | 3 | -11 ± 56 |
| | Night | 142 | -0.10 ± 0.14 | 426 | -0.29 ± 0.30 | 140 | 0.038 ± 0.029 | 1 | -4 |
| Cycle 2 | Day | 312 | -0.13 ± 0.12 | 972 | -0.14 ± 0.19 | 324 | 0.011 ± 0.012 | 4 | -12 ± 19 |
| | Night | 180 | 0.28 ± 0.18 | 559 | -0.15 ± 0.29 | 184 | -0.002 ± 0.012 | 2 | 7 |
| Cycle 3 | Day | 365 | -0.08 ± 0.24 | - | - | 141 | 0.013 ± 0.012 | 4 | -22 ± 22 |
| | Night | 132 | -1.34 ± 0.77 | - | - | 53 | -0.026 ± 0.009 | 2 | -8 |

3.4. Biogeochemical processes variability across diel cycles

To assess the variability of biogeochemical processes during the diel cycle, we present time series of temperature, salinity, and pH_{T25} (Figure 5). In the time series, large fluctuations were primarily observed in the SML, particularly during the day. This increased variability is consistent with the patterns described in the previous section, although the standard deviations between SML and ULW are similar overall (Table S2). The changes during the day occurred rapidly, with increases and decreases spanning 3-5-minute intervals for the three parameters. More specifically, during sampling at 18:00 UTC of Cycle 2, we recorded variations over brief intervals, specifically showing changes of approximately 0.28 °C in temperature, 0.30 g kg⁻¹ in salinity, and 0.016 units in pH_{T25}. During the night, fluctuations were less frequent and of smaller magnitude, except for a sudden change at the end of the sampling conducted at 02:00 UTC in Cycle 2. At that point, there was a slight increase in pH_{T25} at both SML and ULW, along with a decrease in salinity at both depths. This observation suggests that daytime surface heating, evaporation, and production processes likely result in changes in temperature, salinity, and pH_{T25}, which are less pronounced at night.

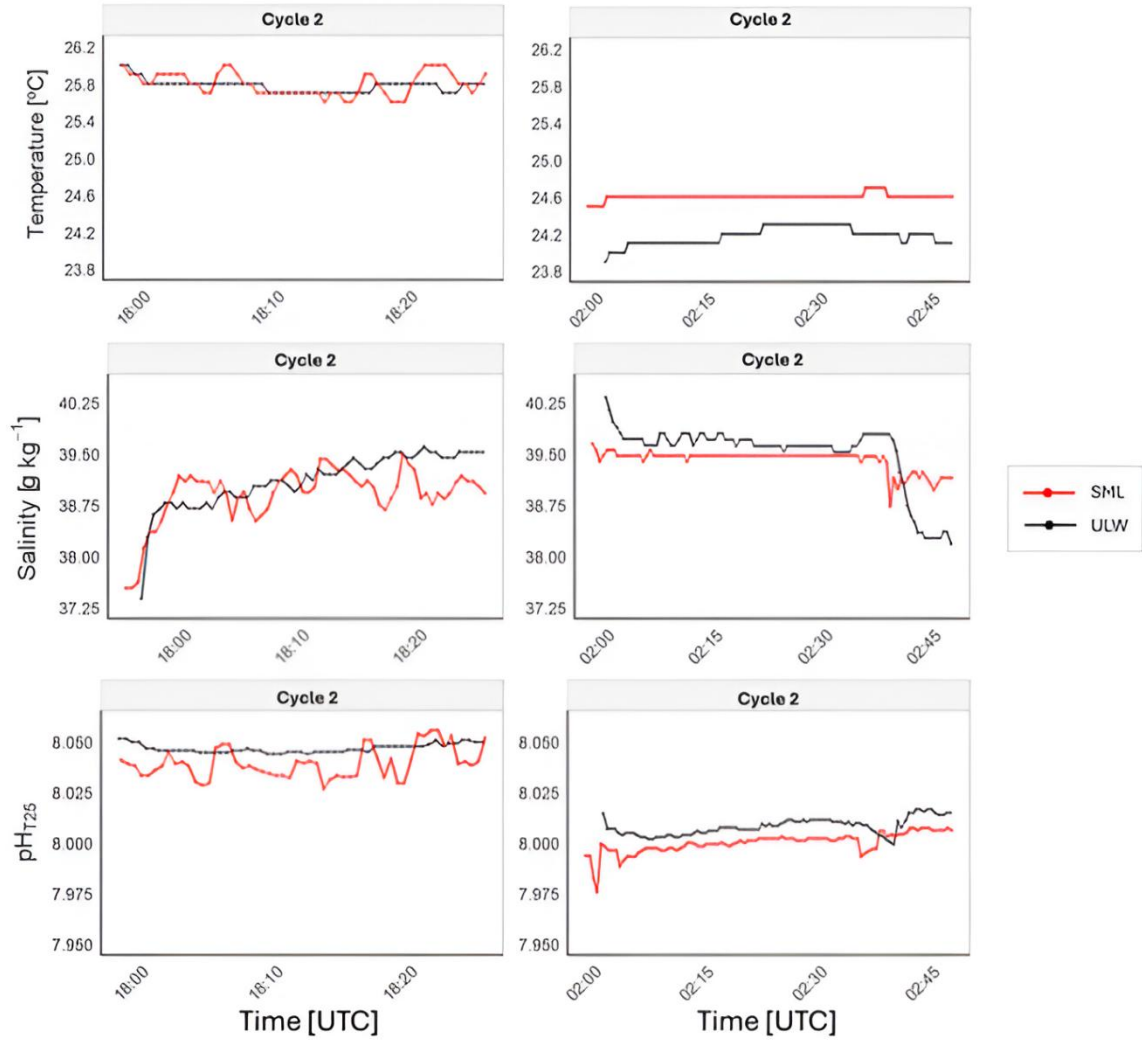


Figure 5. Time series data of temperature, salinity, and $\text{pH}_{\text{T}25}$ collected during Cycle 2: Diurnal (18:00 UTC, August 12) and Nocturnal (02:00 UTC, August 13) measurements.

To assess the variability observed in the SML, the σ_t time series for Cycle 2 at 18:00 UTC and 02:00 UTC was plotted (Figure 6), and evaporation rates within the SML were calculated for Cycles 1 and 2 (Table 3), as salinity data required for calculations in Cycle 3 were not available. The σ_t time series throughout the day exhibits greater variability in the SML compared to nocturnal data, when density fluctuations decrease. However, this trend of variability was not observed in the ULW. The observed patterns of temperature, salinity, $\text{pH}_{\text{T}25}$, and σ_t align with the calculated evaporation rates. In Cycles 1 and 2, the evaporation rates peaked at 14:00 UTC (0.043 mm h^{-1} and 0.074 mm h^{-1} , respectively). They remained high during the late afternoon at 18:00 UTC (0.042 mm h^{-1} and 0.041 mm h^{-1} , respectively), coinciding with the periods of highest solar radiation and wind speed (Figure 2). In contrast, the evaporation rate was close to zero at night. This behaviour highlights the influence of meteorological forcing on the SML during the day, underscoring the connection between evaporation and the observed variability.

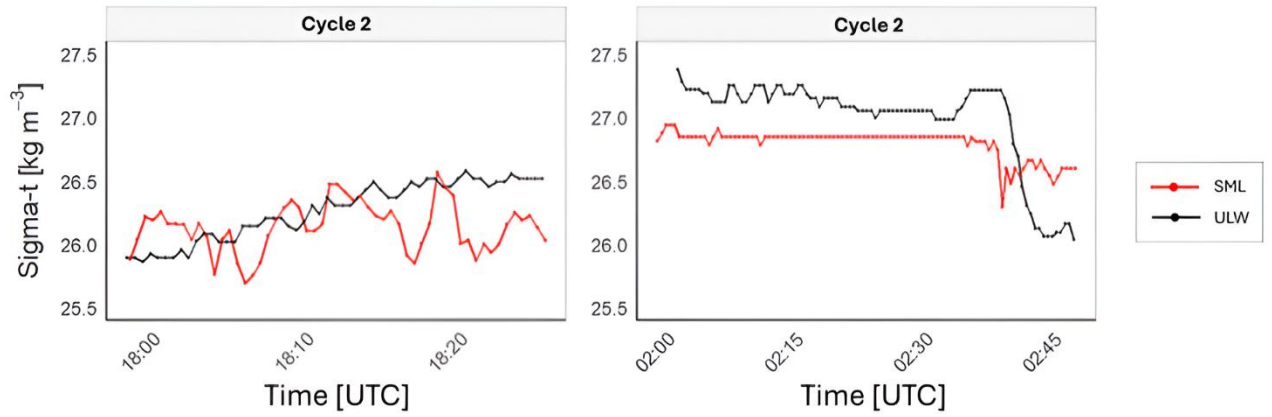


Figure 6. Time series during Cycle 2 for diurnal (18:00 UTC on August 12) and nocturnal (02:00 UTC on August 13) sigma- t data. Sigma- t is defined as the density at a given temperature and salinity minus 1,000 kg m⁻³.

Table 3. Estimated evaporation rates (mm h⁻¹) based on latent heat flux and seawater density in the SML.

| Evaporation rates [mm h ⁻¹] | | | | |
|---|------------|-------|-----------------------|-----|
| Cycle | Time (UTC) | Mean | sd | n |
| Cycle 1 | 06:00 | | | |
| | 10:00 | 0.031 | $1.261 \cdot 10^{-3}$ | 41 |
| | 14:00 | 0.043 | $4.646 \cdot 10^{-4}$ | 67 |
| | 18:00 | 0.042 | $6.674 \cdot 10^{-4}$ | 64 |
| | 22:00 | 0.000 | 0.00 | 66 |
| | 02:00 | 0.000 | 0.00 | 76 |
| Cycle 2 | 06:00 | 0.000 | 0.00 | 68 |
| | 10:00 | 0.012 | $2.040 \cdot 10^{-4}$ | 111 |
| | 14:00 | 0.074 | $1.667 \cdot 10^{-3}$ | 78 |
| | 18:00 | 0.041 | $8.670 \cdot 10^{-4}$ | 55 |
| | 22:00 | 0.000 | 0.00 | 82 |
| | 02:00 | 0.000 | $3.960 \cdot 10^{-6}$ | 98 |

To study the gas exchange between the atmosphere and the ocean, we calculated the CO₂ fluxes and k values using a wind-based parameterisation (Wanninkhof, 2014) for all three cycles and during both day and night (Figure 7). In Cycle 1, despite the limited data, a flux of 3.64 ± 1.15 mmol cm⁻² h⁻¹ was detected during the day, while the flux was close to zero at night. A similar pattern appeared in Cycles 2 and 3, where the fluxes peaked at approximately 14:00 UTC and declined to near zero thereafter. However, the mean flux was higher in Cycle 2 (2.04 ± 3.18 mmol cm⁻² h⁻¹) than in Cycle 3 (0.21 ± 0.28 mmol cm⁻² h⁻¹), consistent with stronger winds. The

average wind speeds during the day were 1.5, 1.9, and 0.4 m s⁻¹ for each cycle, respectively, while at night, winds dropped to nearly 0 m s⁻¹ in the three cycles. The *k* values during the day were 1.12 ± 0.15, 2.22 ± 3.31, and 0.09 ± 0.11 cm h⁻¹, whereas at night, they were close to 0 cm h⁻¹. In this context, excluding nocturnal fluxes in the daily average calculations introduced local percentage errors of 33%, 50%, and 43% for Cycles 1, 2, and 3, respectively. The increased daytime wind speeds enhanced CO₂ fluxes, whereas calm nighttime conditions were associated with reduced or nearly zero gas transfer velocities.

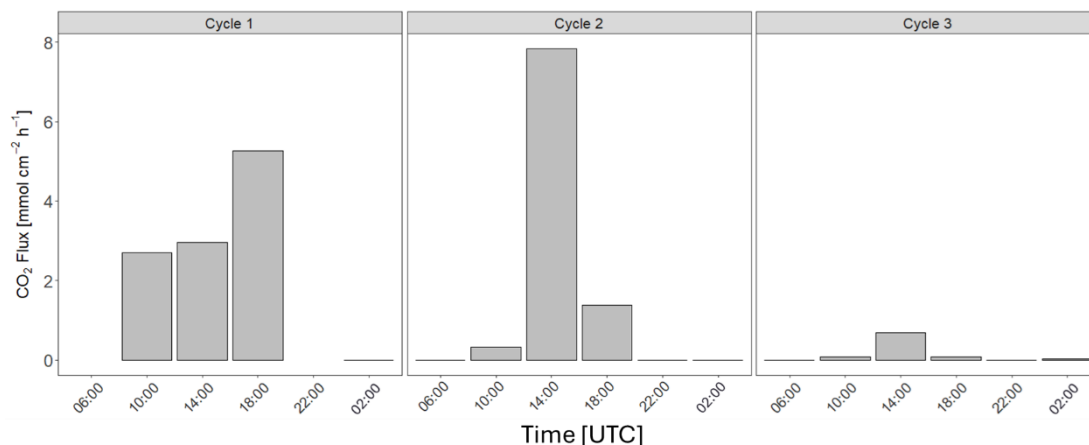


Figure 7. CO₂ fluxes between the atmosphere and the ocean during the studied cycles.

4. Discussion

This study revealed high variability in the SML and ULW during the diel cycle, with significant differences ($p < 0.05$) in temperature, salinity, and pH_{T25} when comparing diurnal and nocturnal data at both depths (Table S1). These results highlight the differences between the meteorological forces that influence the physicochemical properties of seawater during the day and night. For example, during the day, the combined forcing of solar radiation and increased wind speed enhances evaporation rates (Table 3), resulting in the cooling of the SML (Gassen *et al.*, 2023), which drives short-term changes not only in temperature and salinity but also in pH_{T25} (Figure 4). This response reflects the temperature dependence of carbonate speciation (Zeebe & Wolf-Gladrow, 2001). In addition, it is influenced by the combined effect of evaporation, which tends to increase salinity, alkalinity and thus pH_{T25}, and vertical mixing, which can dilute this signal by introducing water with lower pH_{T25} and higher *p*CO₂. This means that the SML is subjected to short-term fluctuations that coincide with changes in wind speed. These fluctuations directly influence thermohaline features, CO₂ system parameters (Acuña *et al.*, 2008), and the kinetics of the metabolic processes occurring in the marine environment (Nimick *et al.*, 2011). Accordingly, in response to the solar photocycle, many marine biogeochemical processes operate on a 24-hour cycle (Nimick *et al.*, 2011), with daily variations comparable in magnitude to the annual variations associated with the amount of solar radiation reaching the ocean surface at different times of the year (Herring *et al.*, 1990; Nimick *et al.*, 2011).

Regarding the variability observed during the day and night, we detected differences in the diurnal temperature data, reaching up to +1.89 °C in the SML and +1.36 °C in the ULW. The calculated mean temperature values

correspond to the Middle Adriatic Surface Water mass (Table S1). Previous studies have reported mean summertime temperatures in the SML of 25.1 °C (Frka *et al.*, 2009) and 27.4 ± 2.9 °C (Milinković *et al.*, 2022). Interestingly, the negative diurnal SML anomalies in Cycles 2 and 3 differ from the typical low-wind patterns (Wurl *et al.*, 2019), suggesting that localised mixing or evaporative cooling may have offset surface warming. In our study, strong stratification combined with weak winds likely promoted localised evaporative cooling and convection, offsetting the expected surface warming, as described in previous studies of near-surface instabilities (Cronin & Sprintall, 2009; Soloviev & Lukas, 2013). Similarly, the observed negative salinity anomaly in the SML could also be linked to these processes. While evaporation driven by intense solar radiation tends to increase salinity in the SML (Frka *et al.*, 2009; Wurl *et al.*, 2019), the consistently negative salinity anomalies observed in Cycles 1 and 2 (Table 2) suggest active vertical mixing, most likely associated with convective processes. This explains the daily variability in salinity distribution between the SML and ULW, with mean values of 39.09 ± 0.33 g kg⁻¹ and 39.15 ± 0.34 g kg⁻¹, respectively.

In this context, the contribution of external forcing factors, such as river discharge, precipitation, and tides, to the observed diurnal variability appears to be minimal. The Krka River has the highest outflow rates in the region, but it typically experiences lower discharge in the summer. This seasonal decrease in freshwater input contributes to the higher salinity values observed in both the SML and ULW compared to periods of stronger river discharge (Frka *et al.*, 2009; Marcinek *et al.*, 2020). Submarine groundwater discharge is also minor, between 0.19-0.31 m³ s⁻¹ during dry periods (Liu *et al.*, 2019), compared to its annual mean of 52.9 m³ s⁻¹ (Bužančić *et al.*, 2016; Marcinek *et al.*, 2020). In addition, precipitation during the first half of August 2020 was very low, averaging 1.4 mm (Croatian Meteorological and Hydrological Service, 2020), further limiting freshwater input and variability in river flow. Similarly, tidal effects at this location are minimal, characterised by a microtidal range of 0.2 to 0.5 meters (Cukrov, Cindrić, et al., 2024). Given the stable stratification of the estuary, such small tidal amplitudes are insufficient to generate significant tidally driven vertical mixing. Instead, the observed variability can be explained by localised near-surface mixing linked to evaporation, density instabilities, and short-term turbulence at the air–sea interface. Furthermore, the observed variability follows a diurnal (24-hour) cycle rather than a semi-diurnal (12-hour) cycle, reinforcing the interpretation that the patterns are primarily driven by surface warming and evaporation rather than tidal forcing (Wurl *et al.*, 2019). This contrasts with mesotidal environments (e.g., Stolle *et al.*, 2020), where tidal mixing complicates the detection of diurnal variability, highlighting the advantage of studying these processes in microtidal settings such as the Adriatic.

The interaction between biological processes and the physicochemical properties of seawater is complex (Álvarez *et al.*, 2014; Cantoni *et al.*, 2012) and has a delicate balance in the marine environment (Cantoni *et al.*, 2012; Takahashi *et al.*, 2002). This interaction directly influences biogeochemical processes typically regulated by production and respiration (Poulson & Sullivan, 2010). These processes significantly affect the pH of seawater through the uptake or removal of CO₂. During the day, photosynthesis lowers *p*CO₂ levels and increases pH by consuming CO₂, whereas at night, CO₂ from respiration accumulates, increasing *p*CO₂ and decreasing pH (Cantoni *et al.*, 2012). However, as we can see in Cycle 3 (Table S2), the observed increase in *p*CO₂ (525 ± 47 µatm) and pH_{T25} (8.042 ± 0.020) values during the day compared to those measured at night (465 µatm; 7.993 ± 0.026). This pattern likely reflects biological and mixing dynamics: enhanced respiration and

CO₂ accumulation in the upper layers of the water due to limited mixing may offset the anticipated photosynthetic uptake (Takahashi *et al.*, 2002), while photoinhibition under solar radiation (Feng *et al.*, 2008; Platt *et al.*, 1980) could reduce photosynthesis efficiency. Taken together, these processes provide a plausible explanation for the unexpected daytime increase in *p*CO₂ despite favourable light conditions (Takahashi *et al.*, 2002).

The complexity of the coupled thermohaline and pH dynamics in seawater is highlighted in the time-series results (Figure 5). The observed fluctuations in the SML for temperature, salinity, and pH_{T25} may be due to buoyancy fluxes. Wind, thermohaline fluctuations, precipitation, and evaporation have a significant influence on surface turbulence (Cronin & Sprintall, 2001). The SML absorbs heat from sunlight and cools through radiation and heat loss, leading to changes in temperature and salinity that disrupt buoyancy, cause convective overturning, entrain deeper water from the ULW, and eventually promote mixing (Cronin & Sprintall, 2001). Wind can also enhance this process by creating tangential stress that acts as a vertical momentum flux. Temperature and salinity changes in the SML led to stratification or convection, with mixing, depending on oceanic and atmospheric forcing (Figure 5). This process has already been observed in the SML (Wurl *et al.*, 2019) and was found to regulate buoyancy fluxes through evaporative salinisation, playing a crucial role in the exchange of climate-relevant gases and heat between the ocean and the atmosphere.

In this context, the existence of these buoyancy fluxes only during the day could also explain the diel difference in CO₂ exchange between the atmosphere and the ocean. As observed in this study, the CO₂ fluxes exhibited differences between daytime ($1.94 \pm 2.45 \text{ mmol cm}^{-2} \text{ h}^{-1}$) and nighttime ($0.01 \pm 0.01 \text{ mmol cm}^{-2} \text{ h}^{-1}$) conditions. This pattern is consistent with the strong dependence of the gas transfer velocity (*k*) on wind forcing (Wanninkhof, 2014), confirming that wind is the dominant driver of diel variability. In addition, daytime buoyancy fluxes, enhanced by wind-driven evaporation and density instabilities, may further facilitate CO₂ exchange during the day, amplifying the effect of wind. Additionally, the absence of wind at night reduced the calculated flux to nearly zero. This observation is consistent with previous suggestions that gas transfer velocity parameterisations without an intercept may underestimate conditions in very calm waters (Ribas-Ribas *et al.*, 2019). Other processes, such as small-scale convection or vertical *p*CO₂ gradients in the upper water column (Liss & Merlivat, 1986; Stolle *et al.*, 2020), may also modulate short-term variability, but their contribution in our dataset appears minor compared to wind forcing. At the same time, SML properties themselves may contribute: slightly lower temperature and salinity enhance CO₂ solubility, while reduced turbulence at the boundary layer further limits exchange. The main implication of our results is that neglecting nocturnal fluxes leads to a systematic bias: the three diel cycles were overestimated by 33%, 50%, and 44%, respectively. Thus, while wind remains the principal driver, including nighttime measurements is essential to avoid biased daily estimates.

5. Conclusions

This study observed a clear diel variability in the distribution of thermohaline features and variables describing the marine inorganic carbon cycle, including temperature, salinity, pH_{T25}, and *p*CO₂. The SML experiences pronounced fluctuations in these parameters throughout the day, influenced by daily changes, like solar radiation, which directly affect the described variables and the environment's metabolic activity. In addition, higher CO₂

fluxes were observed during the day, coinciding with increased wind speeds and buoyancy fluxes that enhanced the exchange of CO₂ between the two compartments. Thus, by emphasising the study of diel cycles, it has been observed that the daily variability of biogeochemical processes is in a delicate balance, making it challenging to obtain a comprehensive global understanding of marine chemistry. Technological advances have been made in sampling equipment for short temporal and spatial scales over the past few decades. However, such progress has not been extended to nighttime observations, which remain significantly more challenging due to the greater logistical complexity and heightened safety considerations associated with operating aboard oceanographic vessels at night. In this context, it is essential to study complete diel cycles, which are crucial for understanding the global carbon budget and its associated uncertainties. Thus, generating a network of diurnal cycle data will identify the drivers of changes in marine chemistry, allowing for the assessment of the responses of marine ecosystems in the context of climate change.

Data Availability Statements

The datasets supporting the findings of this study are available at PANGAEA. The diel variability dataset is accessible at <https://doi.pangaea.de/10.1594/PANGAEA.984017> (Ribas-Ribas *et al.*, 2023a). Additional supporting datasets include meteorological data (<https://doi.pangaea.de/10.1594/PANGAEA.984331>; Ribas-Ribas *et al.*, 2023b), discrete bottle samples (<https://doi.pangaea.de/10.1594/PANGAEA.984018>; Ribas-Ribas *et al.*, 2023c), and high-frequency measurements (<https://doi.pangaea.de/10.1594/PANGAEA.984020>; Ribas-Ribas *et al.*, 2023d).

Acknowledgements

This work was funded by the German Research Foundation (DFG), project number 427614800, and by the Croatian Science Foundation under the project IP-2018-01-3105: *Biochemical Responses of Oligotrophic Adriatic Surface Ecosystems to Atmospheric Deposition Inputs* (BiREADI). It was also supported by the German Academic Exchange Service (DAAD) under project 57513644: *Diurnal Dynamics at the Sea-Atmosphere Interface (INSIST)*. Additionally, the author gratefully acknowledges the support from the Erasmus+ KA 131 SMP OUT program (2022-2023) for funding a research internship at the Carl von Ossietzky Universität Oldenburg - Institut für Chemie und Biologie des Meeres (ICBM). The authors thank Carola Lehnert, Brandy T. Robinson, and Lisa Gassen for operating the sea surface scanner and conducting SML sampling, Carmen Cöhr for initial S³ data treatment, and Leonie Jaeger for assistance with the evaporation rate calculations.

Author Contribution

AL-P: Data Curation, Formal Analysis, Methodology, Visualization, Writing – Original Draft, Writing – Review & Editing. **OW:** Funding Acquisition, Resources, Formal Analysis, Writing – Review & Editing. **SF:** Funding Acquisition, Resources, Formal Analysis, Writing – Review & Editing. **MR-R:** Conceptualisation, Formal Analysis, Visualization, Funding Acquisition, Resources, Supervision, Writing – Original Draft, Writing – Review & Editing.

References

- Acuña, V., Wolf, A., Uehlinger, U., & Tockner, K.: Temperature dependence of stream benthic respiration in an alpine river network under global warming, *Freshw. Biol.*, 53, 2076–2088, <https://doi.org/10.1111/j.1365-2427.2008.02028.x>, 2008.
- Álvarez, M., Sanleón-Bartolomé, H., Tanhua, T., Mintrop, L., Luchetta, A., Cantoni, C., Schroeder, K., & Civitarese, G.: The CO₂ system in the Mediterranean Sea: a basin wide perspective, *Ocean Sci.*, 10, 69–92, <https://doi.org/10.5194/os-10-69-2014>, 2014.
- Álvarez-Rodríguez, M.: The CO₂ system observations in the Mediterranean Sea: past, present and future, in: Designing Med-SHIP: a program for repeated oceanographic surveys, CIESM Workshop Monographs, No. 43, edited by: Briand, F., CIESM, Monaco, pp. 41–50, <https://ciesm.org/catalog/index.php?article=1043>, 2012.
- Bergamasco, A., & Malanotte-Rizzoli, P.: The circulation of the Mediterranean Sea: a historical review of experimental investigations, *Adv. Oceanogr. Limnol.*, 1, 11–28, <https://doi.org/10.1080/19475721.2010.491656>, 2010.
- Borges, A. V.: Do we have enough pieces of the jigsaw to integrate CO₂ fluxes in the coastal ocean?, *Estuaries*, 28, 3–27, <https://doi.org/10.1007/BF02732750>, 2005.
- Brutsaert, W.: Evaporation into the Atmosphere: Theory, History and Applications, Environmental Fluid Mechanics, Springer, Dordrecht, Netherlands, 302 pp., <https://doi.org/10.1007/978-94-017-1497-6>, 2013.
- Bužančić, M., Gladan, Ž. N., Marasović, I., Kušpilić, G., & Grbec, B.: Eutrophication influence on phytoplankton community composition in three bays on the eastern Adriatic coast, *Oceanologia*, 58, 302–316, <https://doi.org/10.1016/j.oceano.2016.05.003>, 2016.
- Cantoni, C., Luchetta, A., Celio, M., Cozzi, S., Raicich, F., & Catalano, G.: Carbonate system variability in the Gulf of Trieste (North Adriatic Sea), *Estuarine, Coastal Shelf Sci.*, 115, 51–62, <https://doi.org/10.1016/j.ecss.2012.07.006>, 2012.
- Cantoni, C., Luchetta, A., Chiggiato, J., Cozzi, S., Schroeder, K., & Langone, L.: Dense water flow and carbonate system in the southern Adriatic: A focus on the 2012 event, *Mar. Geol.*, 375, 15–27, <https://doi.org/10.1016/j.margeo.2015.08.013>, 2016.
- Cetinić, I., Viličić, D., Burić, Z., & Olujić, G.: Phytoplankton seasonality in a highly stratified karstic estuary (Krka, Adriatic Sea), *Hydrobiologia*, 555, 31–40, <https://doi.org/10.1007/s10750-005-1107-6>, 2006.
- Croatian Meteorological and Hydrological Service.: Precipitation data for August 2020, available at: <https://meteo.hr>, 2020.

- 490 Cronin, M. F., & Sprintall, J.: Wind-and buoyancy-forced upper ocean, in: Elements of Physical Oceanography: A Derivative of the Encyclopedia of Ocean Sciences, 237–245, <https://doi.org/10.1006/rwos.2001.0157>, 2001.
- Cukrov, N., Cindrić, A.-M., Omanović, D., & Cukrov, N.: Spatial distribution, ecological risk assessment, and source identification of metals in sediments of the Krka River Estuary (Croatia), *Sustainability*, 16, 1800, <https://doi.org/10.3390/su16051800>, 2024a.
- 495 Cukrov, N., Cukrov, N., & Omanović, D.: Early diagenetic processes in the sediments of the Krka River Estuary, *J. Mar. Sci. Eng.*, 12, 466, <https://doi.org/10.3390/jmse12030466>, 2024b.
- Cunliffe, M., Engel, A., Frka, S., Gašparović, B., Guitart, C., Murrell, J. C., Salter, M., Stolle, C., Upstill-Goddard, R., & Wurl, O.: Sea surface microlayers: A unified physicochemical and biological perspective of the air–ocean interface, *Prog. Oceanogr.*, 109, 104–116, <https://doi.org/10.1016/j.pocean.2012.08.004>, 2013.
- 500 De Montety, V., Martin, J. B., Cohen, M. J., Foster, C., & Kurz, M. J.: Influence of diel biogeochemical cycles on carbonate equilibrium in a karst river, *Chem. Geol.*, 283(1–2), 31–43, <https://doi.org/10.1016/j.chemgeo.2010.12.025>, 2011.
- 505 Del Giorgio, P., & Williams, P. (Eds.): *Respiration in Aquatic Ecosystems*, Oxford University Press, Oxford, UK, 320 pp., ISBN 9780198527084, 2005.
- Dickson, A. G., & Millero, F. J.: A comparison of the equilibrium constants for the dissociation of carbonic acid in seawater media, *Deep Sea Res. Part A*, 34(10), 1733–1743, [https://doi.org/10.1016/0198-0149\(87\)90021-5](https://doi.org/10.1016/0198-0149(87)90021-5), 1987.
- 510 Dickson, A. G., Sabine, C. L., & Christian, J. R.: Guide to best practices for ocean CO₂ measurements, PICES Special Publication 3, North Pacific Marine Science Organization, 191 pp., ISBN 1-897176-07-4, 2007.
- Doney, S. C., Fabry, V. J., Feely, R. A., & Kleypas, J. A.: Ocean Acidification: The Other CO₂ Problem, *Annu. Rev. Mar. Sci.*, 1(1), 169–192, <https://doi.org/10.1146/annurev.marine.010908.163834>, 2009.
- Engel, A., Bange, H. W., Cunliffe, M., Burrows, S. M., Friedrichs, G., Galgani, L., Herrmann, H., Hertkorn, N., Johnson, M., Liss, P. S., Quinn, P. K., Schartau, M., Soloviev, A., Stolle, C., Upstill-Goddard, R. C., Van Pinxteren, M., & Zäncker, B.: The ocean’s vital skin: toward an integrated understanding of the sea surface microlayer, *Front. Mar. Sci.*, 4, 165, <https://doi.org/10.3389/fmars.2017.00165>, 2017.
- 515 Fanning, K. A., & Pilson, Michael.: On the Spectrophotometric determination of dissolved silica in natural waters, *Anal. Chem.*, 45(1), 136–140, <https://doi.org/10.1021/ac60323a021>, 1973.

- 520 Feng, Y., Warner, M. E., Zhang, Y., Sun, J., Fu, F.-X., Rose, J. M., & Hutchins, D. A.: Interactive effects of increased pCO₂, temperature and irradiance on the marine coccolithophore *Emiliania huxleyi* (Prymnesiophyceae), *Eur. J. Phycol.*, 43(1), 87–98, <https://doi.org/10.1080/09670260701664674>, 2008.
- Friedlingstein, P., O’Sullivan, M., Jones, M. W., Andrew, R. M., Hauck, J., Landschützer, P., Le Quéré, C., Li, H., Luijkx, I. T., & Olsen, A.: Global carbon budget 2024, *Earth Syst. Sci. Data*, 17, 965–1098, <https://doi.org/10.5194/essd-17-965-2025>, 2024.
- 525 Frka, S., Kozarac, Z., & Čosović, B.: Characterization and seasonal variations of surface active substances in the natural sea surface micro-layers of the coastal Middle Adriatic stations, *Estuar. Coast. Shelf Sci.*, 85(4), 555–564, <https://doi.org/10.1016/j.ecss.2009.09.023>, 2009.
- Garbe, C. S., Rutgersson, A., Boutin, J., De Leeuw, G., Delille, B., Fairall, C. W., Gruber, N., Hare, J., Ho, D. T., Johnson, M. T., Nightingale, P. D., Pettersson, H., Piskozub, J., Sahlée, E., Tsai, W., Ward, B., Woolf, D. K., & Zappa, C. J.: Transfer across the air–sea interface, in: *Ocean–Atmosphere Interactions of Gases and Particles*, edited by: Liss, P. S. and Johnson, M. T., Springer, Berlin, Heidelberg, Germany, 55–112, https://doi.org/10.1007/978-3-642-25643-1_2, 2014.
- 530 Garbe, C. S., Rutgersson, A., Boutin, J., De Leeuw, G., Delille, B., Fairall, C. W., Gruber, N., Hare, J., Ho, D. T., Johnson, M. T., Nightingale, P. D., Pettersson, H., Piskozub, J., Sahlée, E., Tsai, W., Ward, B., Woolf, D. K., & Zappa, C. J.: Transfer across the air–sea interface, in: *Ocean–Atmosphere Interactions of Gases and Particles*, edited by: Liss, P. S. and Johnson, M. T., Springer, Berlin, Heidelberg, Germany, 55–112, https://doi.org/10.1007/978-3-642-25643-1_2, 2014.
- Gassen, L., Badewien, T. H., Ewald, J., Ribas-Ribas, M., & Wurl, O.: Temperature and Salinity Anomalies in the Sea Surface Microlayer of the South Pacific during Precipitation Events, *J. Geophys. Res. Oceans*, e2023JC019638, <https://doi.org/10.1029/2023JC019638>, 2023.
- 535 Gassen, L., Badewien, T. H., Ewald, J., Ribas-Ribas, M., & Wurl, O.: Temperature and Salinity Anomalies in the Sea Surface Microlayer of the South Pacific during Precipitation Events, *J. Geophys. Res. Oceans*, e2023JC019638, <https://doi.org/10.1029/2023JC019638>, 2023.
- Gattuso, J.-P., Allemand, D., & Frankignoulle, M.: Photosynthesis and calcification at cellular, organismal and community levels in coral reefs: a review on interactions and control by carbonate chemistry, *Am. Zool.*, 39, 160–183, <https://doi.org/10.1093/icb/39.1.160>, 1999.
- 540 Gattuso, J.-P., Magnan, A., Billé, R., Cheung, W. W. L., Howes, E. L., Joos, F., Allemand, D., Bopp, L., Cooley, S. R., Eakin, C. M., Hoegh-Guldberg, O., Kelly, R. P., Pörtner, H.-O., Rogers, A. D., Baxter, J. M., Laffoley, D., Osborn, D., Rankovic, A., Rochette, J., ... Turley, C.: Contrasting futures for ocean and society from different anthropogenic CO₂ emissions scenarios, *Science*, 349(6243), aac4722, <https://doi.org/10.1126/science.aac4722>, 2015.
- 545 Hassoun, A. E. R., Bantelman, A., Canu, D., Comeau, S., Galdies, C., Gattuso, J.-P., Giani, M., Grelaud, M., Hendriks, I. E., Ibello, V., Idrissi, M., Krasakopoulou, E., Shaltout, N., Solidoro, C., Swarzenski, P. W., & Ziveri, P.: Ocean acidification research in the Mediterranean Sea: Status, trends and next steps, *Front. Mar. Sci.*, 9, 892670, <https://doi.org/10.3389/fmars.2022.892670>, 2022.

- Hassoun, A. E. R., Gemayel, E., Krasakopoulou, E., Goyet, C., Abboud-Abi Saab, M., Guglielmi, V., Touratier, F., & Falco, C.: Acidification of the Mediterranean Sea from anthropogenic carbon penetration, *Deep Sea Res. Part I*, 102, 1–15, <https://doi.org/10.1016/j.dsr.2015.04.005>, 2015.
- Herring, P. J., Campbell, A. K., Whitfeld, M., & Maddock, L. (Eds.): *Light and Life in the Sea*, Cambridge University Press, Cambridge, UK, 366 pp., ISBN 978-0521392075, 1990.
- Hoegh-Guldberg, O., Cai, R., Poloczanska, E. S., Brewer, P. G., Sundby, S., Hilmi, K., Fabry, V. J., Jung, S., Skirving, W., & Stone, D. A.: The ocean, in: *Climate Change 2014: Impacts, Adaptation, and Vulnerability. Part B: Regional Aspects*, edited by: Barros, V. R., Field, C. B., Dokken, D. J., Mastrandrea, M. D., Mach, K. J., Bilir, T. E., Chatterjee, M., Ebi, K. L., Estrada, Y. O., Genova, R. C., Girma, B., Kissel, E. S., Levy, A. N., MacCracken, S., Mastrandrea, P. R., and White, L. L., Cambridge University Press, Cambridge, United Kingdom and New York, NY, USA, 1655–1731, <https://doi.org/10.1017/CBO9781107415386.026>, 2014.
- Humphreys, M. P., Lewis, E. R., Sharp, J. D., & Pierrot, D.: PyCO2SYS v1.8: Marine carbonate system calculations in Python, *Geoscientific Model Development*, 15(1), 15–43, <https://doi.org/10.5194/gmd-15-15-2022>, 2022.
- IPCC: *Climate Change 2021 – The Physical Science Basis, Contribution of Working Group I to the Sixth Assessment Report of the Intergovernmental Panel on Climate Change*, Cambridge University Press, Cambridge, United Kingdom and New York, NY, USA, <https://doi.org/10.1017/9781009157896>, 2023.
- Kapsenberg, L., Alliouane, S., Gazeau, F., Mousseau, L., & Gattuso, J.-P.: Coastal ocean acidification and increasing total alkalinity in the northwestern Mediterranean Sea, *Ocean Sci.*, 13, 411–426, <https://doi.org/10.5194/os-13-411-2017>, 2017.
- Kittel, C., & Kroemer, H.: *Thermal Physics*, Macmillan, ISBN 978-0716710882, 1980.
- Laskov, C., Herzog, C., Lewandowski, J., & Hupfer, M.: Miniaturized photometrical methods for the rapid analysis of phosphate, ammonium, ferrous iron, and sulfate in pore water of freshwater sediments, *Limnol. Oceanogr. Methods*, 5, 63–71, <https://doi.org/10.4319/lom.2007.5.63>, 2007.
- Lee, K., Kim, T.-W., Byrne, R. H., Millero, F. J., Feely, R. A., & Liu, Y.-M.: The universal ratio of boron to chlorinity for the North Pacific and North Atlantic oceans, *Geochim. Cosmochim. Acta*, 74, 1801–1811, <https://doi.org/10.1016/j.gca.2009.12.027>, 2010.

- Liss, P. S., & Duce, R. A.: The Sea Surface and Global Change, Cambridge University Press, ISBN 9780521562737, 1997.
- 580 Liss, P. S., & Merlivat, L.: Air–sea gas exchange rates: introduction and synthesis, in: The Role of Air–Sea Exchange in Geochemical Cycling, edited by: Buat-Ménard, P., Springer, Dordrecht, Netherlands, 113–127, https://doi.org/10.1007/978-94-009-4738-2_5, 1986.
- Liu, J., Hrutić, E., Du, J., Gašparović, B., Čanković, M., Cukrov, N., Zhu, Z., & Zhang, R.: Net submarine groundwater-derived dissolved inorganic nutrients and carbon input to the oligotrophic stratified karstic estuary of the Krka River (Adriatic Sea, Croatia), *J. Geophys. Res.-Oceans*, 124, 4334–4349, <https://doi.org/10.1029/2018JC014814>, 2019.
- 585 Marcinek, S., Santinelli, C., Cindrić, A.-M., Evangelista, V., Gonnelli, M., Layglon, N., Mounier, S., Lenoble, V., & Omanović, D.: Dissolved organic matter dynamics in the pristine Krka River estuary (Croatia), *Mar. Chem.*, 225, 103848, <https://doi.org/10.1016/j.marchem.2020.103848>, 2020.
- 590 Mehrbach, C., Culberson, C. H., Hawley, J. E., & Pytkowicz, R. M.: Measurement of the apparent dissociation constants of carbonic acid in seawater at atmospheric pressure 1, *Limnol. Oceanogr.*, 18, 897–907, <https://doi.org/10.4319/lo.1973.18.6.0897>, 1973.
- Milinković, A., Penezić, A., Kušan, A. C., Gluščić, V., Žužul, S., Skejić, S., Šantić, D., Godec, R., Pehnec, G., Omanović, D., Engel, A., & Frka, S.: Variabilities of biochemical properties of the sea surface microlayer: Insights to the atmospheric deposition impacts, *Sci. Total Environ.*, 838, 156440, <https://doi.org/10.1016/j.scitotenv.2022.156440>, 2022.
- 595 Mustaffa, N. I. H., Badewien, T. H., Ribas-Ribas, M., & Wurl, O.: High-resolution observations on enrichment processes in the sea-surface microlayer, *Sci. Rep.*, 8, 13122, <https://doi.org/10.1038/s41598-018-31465-8>, 2018.
- 600 Nimick, D. A., Gammons, C. H., & Parker, S. R.: Diel biogeochemical processes and their effect on the aqueous chemistry of streams: A review, *Chem. Geol.*, 283, 3–17, <https://doi.org/10.1016/j.chemgeo.2010.08.017>, 2011.
- Orr, J. C., Fabry, V. J., Aumont, O., Bopp, L., Doney, S. C., Feely, R. A., Gnanadesikan, A., Gruber, N., Ishida, A., Joos, F., Key, R. M., Lindsay, K., Maier-Reimer, E., Matear, R., Monfray, P., Mouchet, A., Najjar, R. G., Plattner, G.-K., Rodgers, K. B., Sabine, C. L., Sarmiento, J. L., Schlitzer, R., Slater, R. D., 605 Totterdell, I. J., Weirig, M.-F., Yamanaka, Y., and Yool, A.: Anthropogenic ocean acidification over the

twenty-first century and its impact on calcifying organisms, *Nature*, 437, 681–686,
<https://doi.org/10.1038/nature04095>, 2005.

Pecci, M., di Sarra, A., Sferlazzo, D., Anello, F., Di Iorio, T., Colella, S., Iaccarino, A., Marullo, S., Meloni, D.,
610 Monteleone, F., Pace, G., & Piacentino, S.: Ocean–atmosphere CO₂ flux at the Lampedusa
Oceanographic Observatory, available at: https://www.lampedusa.enea.it/dataaccess/ocean_co2fluxes,
last access: 19 August 2025, 2023.

Perez, F. F., & Fraga, F.: Association constant of fluoride and hydrogen ions in seawater, *Mar. Chem.*, 21, 161–
168, [https://doi.org/10.1016/0304-4203\(87\)90036-3](https://doi.org/10.1016/0304-4203(87)90036-3), 1987.

615 IPCC Special Report on the Ocean and Cryosphere in a Changing Climate, edited by: Pörtner, H.-O., Roberts, D.
C., Masson-Delmotte, V., Zhai, P., Tignor, M., Poloczanska, E., Mintenbeck, K., Nicolai, M., Okem, A.,
Petzold, J., Rama, B., and Weyer, N. M., Cambridge University Press, Cambridge, UK and New York,
NY, USA, 755 pp., <https://doi.org/10.1017/9781009157964>, 2019.

Poulson, S. R., & Sullivan, A. B.: Assessment of diel chemical and isotopic techniques to investigate
620 biogeochemical cycles in the upper Klamath River, Oregon, USA, *Chem. Geol.*, 269, 3–11,
<https://doi.org/10.1016/j.chemgeo.2009.05.016>, 2010.

Prohić, E., & Juračić, M.: Heavy metals in sediments – problems concerning determination of the anthropogenic
influence: study in the Krka River estuary, eastern Adriatic coast, Yugoslavia, *Environ. Geol. Water Sci.*,
13, 145–151, <https://doi.org/10.1007/BF01665136>, 1989.

625 Ribas-Ribas, M., Battaglia, G., Humphreys, M. P., & Wurl, O.: Impact of nonzero intercept gas transfer velocity
parameterizations on global and regional ocean–atmosphere CO₂ fluxes, *Geosciences*, 9, 230,
<https://doi.org/10.3390/geosciences9050230>, 2019.

Ribas-Ribas, M., Hamizah Mustaffa, N. I., Rahlff, J., Stolle, C., & Wurl, O.: Sea Surface Scanner (S³): A
catamaran for high-resolution measurements of biogeochemical properties of the sea surface
630 microlayer, *J. Atmos. Oceanic Technol.*, 34, 1433–1448, <https://doi.org/10.1175/JTECH-D-17-0017.1>,
2017.

Robinson, A. R., & Golnaraghi, M.: The Physical and Dynamical Oceanography of the Mediterranean Sea, in:
Ocean Processes in Climate Dynamics: Global and Mediterranean Examples, edited by: Malanotte-
Rizzoli, P. and Robinson, A. R., Springer Netherlands, 255–306, [https://doi.org/10.1007/978-94-011-](https://doi.org/10.1007/978-94-011-0870-6_12)
635 0870-6_12, 1994.

Schneider, A., Tanhua, T., Körtzinger, A., & Wallace, D. W. R.: High anthropogenic carbon content in the eastern Mediterranean, *J. Geophys. Res.: Oceans*, 115, C12, <https://doi.org/10.1029/2010JC006171>, 2010.

Sharp, J. D., Pierrot, D., Humphreys, M. P., Epitalon, J.-M., Orr, J. C., Lewis, E. R., & Wallace, D. W. R.: CO2SYSv3 for MATLAB (v3.1), Zenodo [code], <https://doi.org/10.5281/ZENODO.4023039>, 2020

640 Shaw, E. C., McNeil, B. I., & Tilbrook, B.: Impacts of ocean acidification in naturally variable coral reef flat ecosystems, *J. Geophys. Res.-Oceans*, 117, C03038, <https://doi.org/10.1029/2011JC007655>, 2012.

Soloviev, A., & Lukas, R.: *The Near-Surface Layer of the Ocean: Structure, Dynamics and Applications*, 2nd Edn., Springer, Dordrecht, the Netherlands, 572 pp., <https://doi.org/10.1007/978-94-007-7620-8>, 2013.

645 Stolle, C., Ribas-Ribas, M., Badewien, T. H., Barnes, J., Carpenter, L. J., Chance, R., Damgaard, L. R., Durán Quesada, A. M., Engel, A., Frka, S., Galgani, L., Gašparović, B., Gerriets, M., Hamizah Mustaffa, N. I., Herrmann, H., Kallajoki, L., Pereira, R., Radach, F., Revsbech, N. P., and Wurl, O.: The MILAN campaign: studying diel light effects on the air–sea interface, *Bull. Am. Meteorol. Soc.*, 101, E146–E166, <https://doi.org/10.1175/BAMS-D-17-0329.1>, 2020.

650 Takahashi, T., Sutherland, S. C., Chipman, D. W., Goddard, J. G., Ho, C., Newberger, T., Sweeney, C., & Munro, D. R.: Climatological distributions of pH, $p\text{CO}_2$, total CO_2 , alkalinity, and CaCO_3 saturation in the global surface ocean, and temporal changes at selected locations, *Mar. Chem.*, 164, 95–125, <https://doi.org/10.1016/j.marchem.2014.06.004>, 2014.

655 Takahashi, T., Sutherland, S. C., Sweeney, C., Poisson, A., Metzl, N., Tilbrook, B., Bates, N., Wanninkhof, R., Feely, R. A., Sabine, C., Olafsson, J., & Nojiri, Y.: Global sea–air CO_2 flux based on climatological surface ocean $p\text{CO}_2$, and seasonal biological and temperature effects, *Deep Sea Res. Part II: Topical Stud. Oceanogr.*, 49(9–10), 1601–1622, [https://doi.org/10.1016/S0967-0645\(02\)00003-6](https://doi.org/10.1016/S0967-0645(02)00003-6), 2002.

RStudio Team: RStudio: integrated development environment for R, Posit Software, Boston, MA, USA, [software], <https://posit.co/>, 2023.

660 Van Heuven, S., Pierrot, D., Rae, J. W. B., Lewis, E., & Wallace, D. W. R.: MATLAB Program Developed for CO_2 System Calculations, [software], https://doi.org/10.3334/cdiac/otg.co2sys_matlab_v1.1, 2011.

Wanninkhof, R.: Relationship between wind speed and gas exchange over the ocean revisited, *Limnol. Oceanogr.: Methods*, 12(6), 351–362, <https://doi.org/10.4319/lom.2014.12.351>, 2014.

665 Wong, P. P., Losada, I. J., Gattuso, J.-P., Hinkel, J., Khattabi, A., McInnes, K. L., Saito, Y., and Sallenger, A.: Coastal systems and low-lying areas, in: *Climate Change 2014: Impacts, Adaptation, and Vulnerability. Part A: Global and Sectoral Aspects*, Contribution of Working Group II to the Fifth Assessment Report

of the Intergovernmental Panel on Climate Change, edited by: Field, C. B., Barros, V. R., Dokken, D. J., Mach, K. J., Mastrandrea, M. D., Bilir, T. E., Chatterjee, M., Ebi, K. L., Estrada, Y. O., Genova, R. C., Girma, B., Kissel, E. S., Levy, A. N., MacCracken, S., Mastrandrea, P. R., and White, L. L., Cambridge University Press, Cambridge, United Kingdom and New York, NY, USA, 361–409, <https://doi.org/10.1017/CBO9781107415379.010>, 2014.

Wurl, O., Ekau, W., Landing, W. M., & Zappa, C. J.: Sea surface microlayer in a changing ocean – a perspective, *Elem. Sci. Anthropocene*, 5, 31, <https://doi.org/10.1525/elementa.228>, 2017.

Wurl, O., Landing, W. M., Mustaffa, N. I. H., Ribas-Ribas, M., Witte, C. R., & Zappa, C. J.: The Ocean's Skin Layer in the Tropics, in: *Journal of Geophysical Research: Oceans*, 124(1), 59–74, <https://doi.org/10.1029/2018JC014021>, 2019.

Wurl, O., Wurl, E., Miller, L., Johnson, K., & Vagle, S.: Formation and global distribution of sea-surface microlayers, in: *Biogeosciences*, 8(1), 121–135, <https://doi.org/10.5194/bg-8-121-2011>, 2011.

Yates, K. K., Dufore, C., Smiley, N., Jackson, C., & Halley, R. B.: Diurnal variation of oxygen and carbonate system parameters in Tampa Bay and Florida Bay, *Mar. Chem.*, 104, 110–124, <https://doi.org/10.1016/j.marchem.2006.12.008>, 2007.

Zeebe, R. E., & Wolf-Gladrow, D. A.: *CO₂ in Seawater: Equilibrium, Kinetics, Isotopes*, Elsevier Oceanography Series, Vol. 65, Elsevier, Amsterdam, ISBN 0444509461, 2001.

Zutic, V., & Legovic, T.: A film of organic matter at the fresh-water/sea-water interface of an estuary, *Nature*, 328, 612–614, <https://doi.org/10.1038/328612a0>, 1987.